 DOI: 10.1002/eji.201546259 Eur. J. Immunol. 2016. 46: 2574–2586

European Journal of Immunology

Immunity to infection

Research Article

Rewiring cellular metabolism via the AKT/mTOR pathway contributes to host defence against *Mycobacterium tuberculosis* in human and murine cells

Ekta Lachmandas[1], Macarena Beigier-Bompadre[2], Shih-Chin Cheng[1], Vinod Kumar[3], Arjan van Laarhoven[1], Xinhui Wang[1,4], Anne Ammerdorffer[1], Lily Boutens[1], Dirk de Jong[5], Thirumala-Devi Kanneganti[6], Mark S. Gresnigt[1], Tom H.M. Ottenhoff[7], Leo A.B. Joosten[1], Rinke Stienstra[1], Cisca Wijmenga[3], Stefan H.E. Kaufmann[2], Reinout van Crevel[1] and Mihai G. Netea[1]

[1] Department of Internal Medicine, Radboud Center for Infectious Diseases, Radboud University Medical Center, Nijmegen, The Netherlands
[2] Department of Immunology, Max Planck Institute for Infection Biology, Berlin, Germany
[3] UMC Groningen University of Groningen, Groningen, The Netherlands
[4] College of Computer, Qinghai Normal University, Xining, China
[5] Department of Gastroenterology, Radboud University Medical Center, Nijmegen, The Netherlands
[6] Department of Immunology, St. Jude Children's Research Hospital, Memphis, TN, USA
[7] Department of Infectious Diseases, Leiden University Medical Centre, Leiden, The Netherlands

Cells in homeostasis metabolize glucose mainly through the tricarboxylic acid cycle and oxidative phosphorylation, while activated cells switch their basal metabolism to aerobic glycolysis. In this study, we examined whether metabolic reprogramming toward aerobic glycolysis is important for the host response to *Mycobacterium tuberculosis* (Mtb). Through transcriptional and metabolite analysis we show that Mtb induces a switch in host cellular metabolism toward aerobic glycolysis in human peripheral blood mononuclear cells (PBMCs). The metabolic switch is TLR2 dependent but NOD2 independent, and is mediated in part through activation of the AKT-mTOR (mammalian target of rapamycin) pathway. We show that pharmacological inhibition of the AKT/mTOR pathway inhibits cellular responses to Mtb both in vitro in human PBMCs, and in vivo in a model of murine tuberculosis. Our findings reveal a novel regulatory layer of host responses to Mtb that will aid understanding of host susceptibility to Mtb, and which may be exploited for host-directed therapy.

Keywords: Glycolysis · Immunometabolism · mTOR · *Mycobacterium tuberculosis* · TLR2

Additional supporting information may be found in the online version of this article at the publisher's web-site

Correspondence: Dr. Mihai G. Netea
e-mail: mihai.netea@radboudumc.nl

Introduction

In the absence of HIV coinfection, it is mostly unknown what determines susceptibility to *Mycobacterium tuberculosis* (Mtb), which accounts for almost two million deaths annually.

Recent studies suggest that immune activation and cellular energy metabolism may be relevant since changes in metabolism profoundly influence cell fate and effector functions. For example, it has been shown that changes in glucose metabolism influence T-cell lineage polarization, innate and adaptive cellular memory and even protein transport, and secretion in response to cellular activation [1–4]. Naïve and tolerant cells appear to primarily rely on the tricarboxylic acid (TCA) cycle and oxidative phosphorylation for metabolizing glucose and generating stores of ATP necessary for cell survival and function. Upon activation however, a switch toward aerobic glycolysis rewires intracellular glucose metabolism [5]. This permits a significant increase in ATP production and, through the pentose phosphate pathway, provides the nucleotides necessary for cell proliferation [6]. Recent studies by Shi et al. and Gleeson et al. have shown that a shift toward glycolysis is an important component of host defence in murine models of tuberculosis [7, 8]. Taking these studies further, we have investigated which cells, receptors, and regulators promote the Mtb-induced switch to glycolysis in humans. We have tested our hypotheses both in in vitro and in vivo experimental models and verified whether such metabolic reprogramming also occurs in patients with active pulmonary TB.

Results

Transcriptome analysis of TB patients and human Mtb-stimulated PBMCs show a shift toward glycolysis

Based on expression of genes coding for glycolysis or TCA cycle pathways, pulmonary TB patients (PTB) could be clearly separated from individuals with latent tuberculosis infection (LTBI) or healthy controls (CON) using principal component analysis of publically sourced human expression data [9] (Fig. 1A and B). Regression analysis on the first component of both groups showed that both pathways were significantly different between LTBI and PTB ($p < 0.001$ for both) groups. Individuals on antituberculosis treatment were spread throughout the plot with untreated cases closer to PTB and those on 12 months of treatment interspersed with the LTBI and CON groups. Analysis of individual genes in the PTB versus CON groups clearly showed an upregulation of glycolysis genes glyceraldehyde-3-phosphate dehydrogenase (GAPDH) and hexokinase-3 (Fig. 1C and D), which returned toward normal following treatment. The opposite was observed for the TCA cycle gene isocitrate dehydrogenase 3 (NAD+) beta (IDHB3B) (Fig. 1E).

We next examined expression of similar metabolic genes in an in vitro model. Similar to the in vivo dataset described above, Mtb-stimulated peripheral blood mononuclear cells (PBMCs) also displayed a strong upregulation of some genes involved in glycolysis and downregulation of some involved in the TCA cycle (Fig. 1F).

Based on the in vitro and in vivo data analyses, an intracellular map was generated to reflect the switch to aerobic glycolysis induced upon Mtb stimulation (Fig. 1G). The general metabolic shift is further supported by altered expression of individual genes. SLC16A3 (solute carrier family 16 monocarboxylate transport MCT, member 3), which encodes a lactate transporter, was significantly upregulated in PTB patients and returned to normal levels upon treatment (Supporting Information Fig. 1A). Conversely, sirtuin 5 (SIRT5), a protein whose activity is directly linked to the energy status of the cell via the cellular NAD^+/NADH ratio, was downregulated in PTB patients and normalized upon treatment (Supporting Information Fig. 1B).

Mtb drives cellular commitment to aerobic glycolysis in human monocytes and macrophages

Monocytes, macrophages, dendritic cells (DCs), T helper (T_H)1, and T_H17 cells use glucose as a substrate for energy production [10]. To determine the commitment to glycolytic metabolism in stimulated monocytes, we analyzed the extracellular acidification rate (ECAR) as an indicator of the glycolytic rate 24 h poststimulation. There was a significant increase in all three baseline measurements and ECAR levels were approximately 3.3-fold higher in Mtb-stimulated cells (Fig. 2A). This increase in ECAR was responsible for a decrease in the oxygen consumption rate (OCR)/ECAR ratio, as previously described for LPS [11] (Supporting Information Fig. 2A), despite a slightly higher OCR (Fig. 2B).

Similarly, macrophages infected with live Mtb or stimulated with Mtb lysate produced increased levels of lactate, one of the hallmarks of glycolysis (Fig. 2C). Additionally, PBMCs challenged with Mtb showed increased glucose consumption (Fig. 2D) and lactate production (Fig. 2E). Generation of lactate requires the oxidation of NADH to cofactor NAD^+ by lactate dehydrogenase. Accordingly, we observed a significant increase in the ratio of NAD^+/NADH in Mtb-stimulated PBMCs (Fig. 2F). Conversely, resting PBMCs displayed a lower NAD+/NADH ratio reflecting cellular metabolism mostly via the TCA cycle rather than glycolysis (Fig. 2F).

Mtb activates AKT and mTOR in human PBMCs

As mammalian target of rapamycin (mTOR) is the master regulator of cell growth, proliferation, and metabolism, [12] and AKT-mediated mTOR activation induces glucose metabolism, [13, 14] we assessed whether Mtb activated the AKT-mTOR pathway (Fig. 3A). Indeed, sensing of the microorganism induced AKT activation, which was inhibited by the phosphatidylinositol-3 kinase (PI-3K) inhibitor wortmannin (Fig. 3B). In addition, p70-S6K and 4E-BP1, two canonical downstream targets of mTOR, were activated upon Mtb stimulation. Purification of $CD14^+$ monocytes and

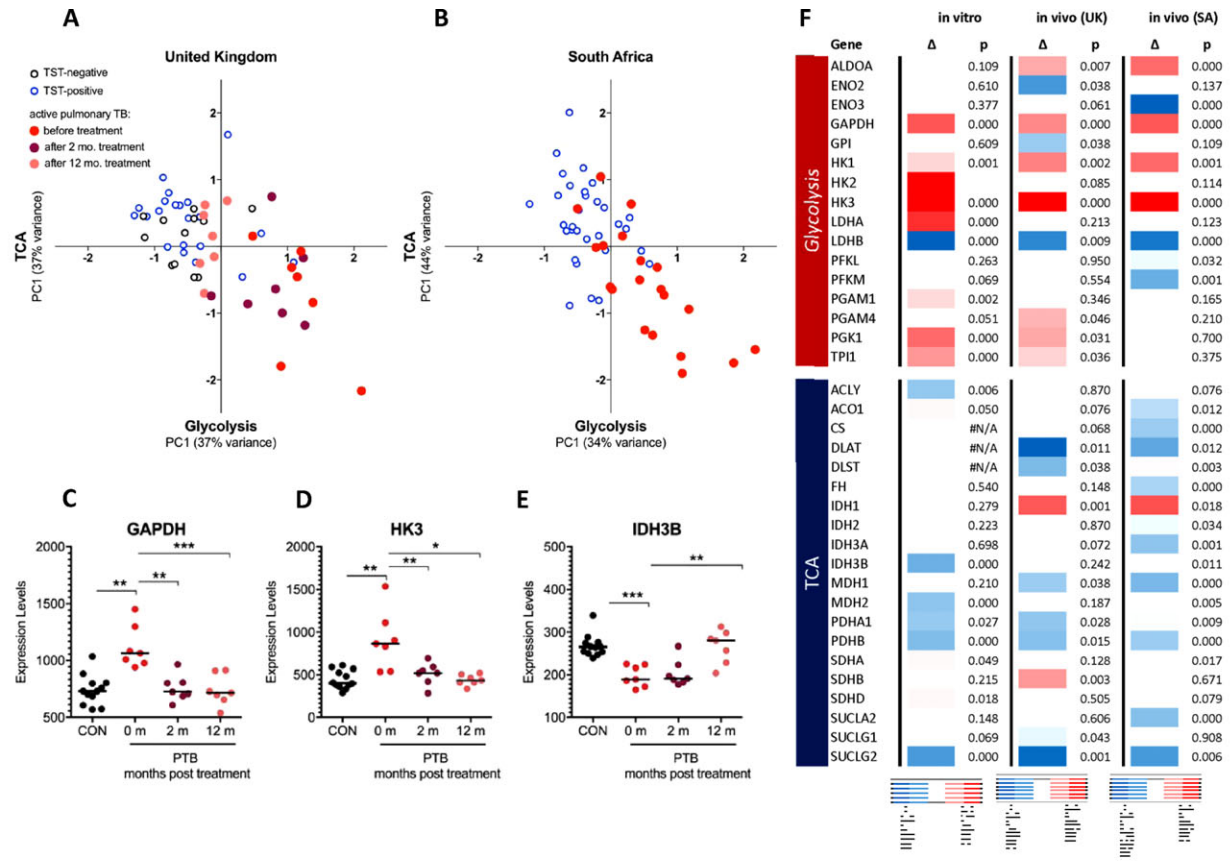

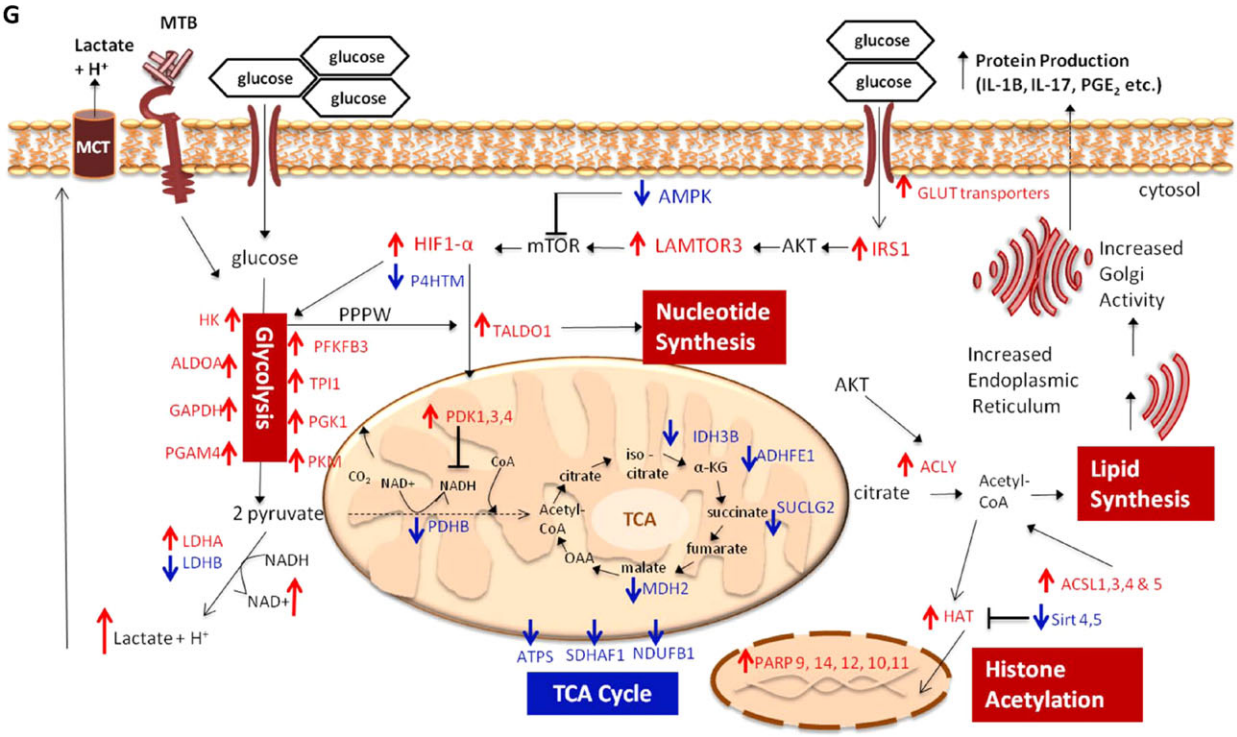

$CD3^+$ T cells from stimulated PBMCs revealed that Mtb induced mTOR activation in monocytes but not T cells (Fig. 3C). Activation of these mTOR targets was inhibited by rapamycin, an mTOR inhibitor, in both PBMCs (Fig. 3D) and $CD14^+$ monocytes (Supporting Information Fig. 3A).

Additionally, rapamycin, torin, and wortmannin significantly decreased lactate release induced by Mtb, further demonstrating the involvement of the mTOR/AKT pathway in induction of glycolysis by Mtb (Fig. 3E–G).

mTOR regulates T_H-cell-derived cytokines from PBMCs in response to Mtb

T lymphocytes form a crucial component of the host defence against Mtb. Direct inhibition of glycolysis by 2-deoxy-glucose led to a dose-dependent decrease in the production of the T_H cytokines interferon gamma (IFN-γ), interleukin (IL) 17, and IL-22 from PBMCs in response to Mtb (Fig. 4A). Direct inhibition of mTOR by rapamycin or torin or indirectly by AICAR (an AMPK activator; Fig. 4B and C), and inhibition of mTOR-dependent HIF-1α activation by ascorbate also resulted in reduced T_H-derived cytokine production (Fig. 4D). IL-10 production in response to Mtb was also significantly inhibited upon mTOR inhibition (Supporting Information Fig. 4A, B, and D). Production of monocyte-derived tumor necrosis factor (TNF) α, IL-6, and IL-1β was mostly reduced upon inhibition of glycolysis with 2-deoxy-glucose (Supporting Information Fig. 4A). Interestingly, production of monocyte-derived cytokines remained mostly unchanged in the presence of rapamycin, torin, and ascorbate (Supporting Information Fig. 4B–D). These inhibitors did not affect cell survival at the time points used for the stimulation experiments (Supporting Information Fig. 5A–E).

Induction of glycolysis by Mtb is TLR2 dependent but NOD2 independent

We next examined which of the main pattern recognition receptors (PRRs) that mediate recognition of Mtb, [15] are necessary for a metabolic switch toward aerobic glycolysis. PBMCs isolated from patients with a complete deficiency in NOD2 showed decreased cytokine production in response to Mtb (Fig. 5A), but no decrease in lactate production (Fig. 5B). In addition, bone marrow (BM) derived macrophages (BMDMs) from NOD2 knockout ($NOD2^{-/-}$) and NOD1/NOD2 double knockout ($NOD1^{-/-}/NOD2^{-/-}$) mice stimulated with Mtb showed decreased KC and IL-6 production. However, as with the NOD2-deficient patients, no change in lactate production was observed and no major differences were apparent after stimulation of BMDMs from NOD1 knockout ($NOD1^{-/-}$) mice either (Fig. 5C and D).

We then examined possible synergy with regard to lactate production between NOD2 and the TLRs involved in recognition of Mtb. As expected, cytokine production of PBMCs stimulated with LPS (TLR4 ligand), Pam3Cys (P3C, TLR2 ligand), or Mtb increased in the presence of muramyl dipeptide (MDP, an NOD2 ligand), while MDP by itself did not induce cytokine production (Fig. 6A and B). On the other hand, MDP showed no synergistic effect for lactate production upon stimulation with the various other TLR ligands (Fig. 6C).

To investigate the role of TLR4 in the induction of aerobic glycolysis by Mtb, we blocked TLR4 by preincubation of PBMCs with *Bartonella quintana* LPS, a potent natural antagonist of TLR4 (Popa et al., [16]), before stimulating with Mtb or *Escherichia coli* LPS. Although a potent decrease in IL-6 and lactate levels was observed for LPS, indicating effective blocking of TLR4, no effect of the TLR4 blockade on Mtb-induced lactate was seen (Fig. 6D and E).

To investigate the role of TLR2, we stimulated BMDMs and peritoneal macrophages from TLR2 knockout ($TLR2^{-/-}$) mice with Mtb and Pam3Cys. Production of KC (IL-8) and lactate was potently decreased in $TLR2^{-/-}$ BMDMs compared to wild-type (WT) controls (Fig. 6F–H). In addition, stimulation of cells isolated from $TLR2^{-/-}$ mice with Mtb led to a decrease in AKT activation compared to controls, while the induction of AKT with insulin, in a TLR-independent manner, was unaffected (Fig. 6I). Collectively, these data implicate TLR2, and not TLR4 or NOD2, as the major PRR that induces AKT/mTOR pathway activation and thus mediates the switch to aerobic glycolysis upon Mtb stimulation.

mTOR inhibition in an in vivo murine experimental model of TB

We then examined the in vivo effects of mTOR inhibition on Mtb-induced cytokine responses. C57BL/6 mice were injected

Figure 1. Transcriptional regulation of glucose metabolism during active TB disease and in PBMCs stimulated with Mtb. (A, B) Principal component analysis of the glycolysis and TCA cycle whole blood gene signatures of microarray data from publically available cohorts from (A) the United Kingdom (UK) and (B) South Africa (SA), previously published by Berry et al. (Series GSE19444) [9]. Data for each sample, including active pulmonary TB (PTB), LTBI (TST positive), and CON (TST negative) individuals were plotted along PC1 for glycolysis versus PC1 for the TCA cycle. For the UK cohort, PC1 accounted for 37% of the total variation for both glycolysis and the TCA cycle. For the SA cohort PC1 accounted for 44 and 34% of the variance for glycolysis and the TCA cycle respectively. (C–E) Individual and mean whole blood gene expression for (C) GAPDH, (D) hexokinase-3, and (E) IDH3B in controls and PTB patients on 0, 2, or 12 months of TB treatment (Series GSE19435). Microarray data derived from Berry et al [9]. Symbols represent individual samples and data are shown as means ± SEM; means were compared using the Mann–Whitney *U* test. $^*p < 0.05$, $^{**}p < 0.01$, $^{***}p < 0.001$. (F) Heatmap of gene expression pattern of glycolysis or TCA cycle genes in in vitro-stimulated PBMCs and in vivo whole blood (UK and SA publically available cohorts). All data was log-2 transformed. The in vitro Mtb stimulations were normalized to RPMI by subtracting means whereas the in vivo PTB cohort was normalized to the corresponding LTBI cohort. *p*-values were considered significant when less than 0.05 as determined by the Wilcoxon signed-rank test for the in vitro data set and by the Mann–Whitney U test for the in vivo data sets. Red represents a significant up regulation, blue a significant down regulation and grey no difference. (G) Schematic representation of upregulated (in red) and downregulated (blue) genes in the glycolysis and TCA cycle pathways as determined by microarray analysis of Mtb-stimulated PBMCs.

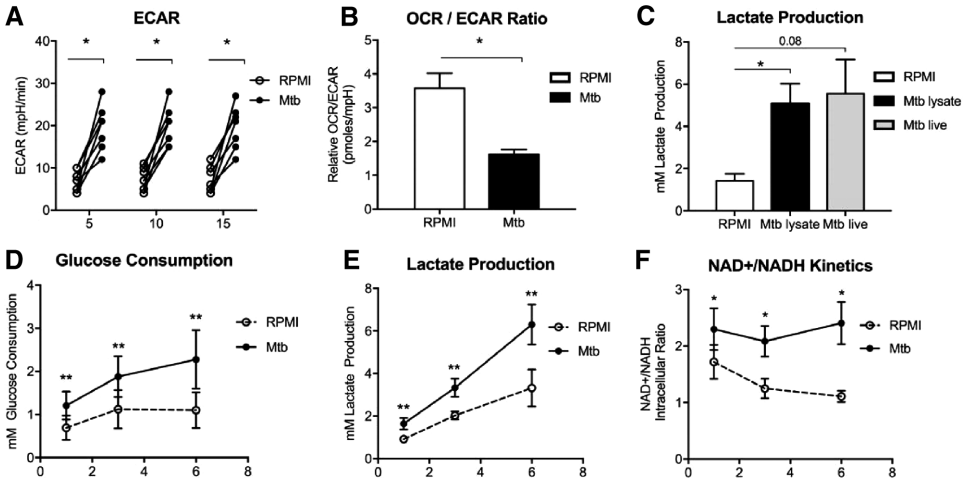

Figure 2. Physiology of the PBMC metabolic response to Mtb stimulation. (A, B) $CD14^+$ monocytes were stimulated for 24 h with Mtb and (A) ECAR and (B) OCR rates were determined using the Seahorse metabolic analyzer. Three baseline measurements were determined. Data are shown as means ± SEM (n = 7). (C) Lactate production from macrophages stimulated with live H37Rv (10:1 MOI) was measured by a fluorescent coupled enzymatic assay. Data are shown as means ± SEM of n = 4, pooled from two independent experiments. (D-F) PBMCs were stimulated with Mtb lysate and the kinetics of (D) glucose consumption, (E) lactate production and (F) the intracellular NAD^+/NADH ratios from days 1, 3 and 7 was measured by metabolite specific coupled enzymatic assays. Data are shown as means ± SEM of n = 6 to 8, pooled from three independent experiments. Means were compared using the Wilcoxon signed-rank test, $^*p < 0.05$).

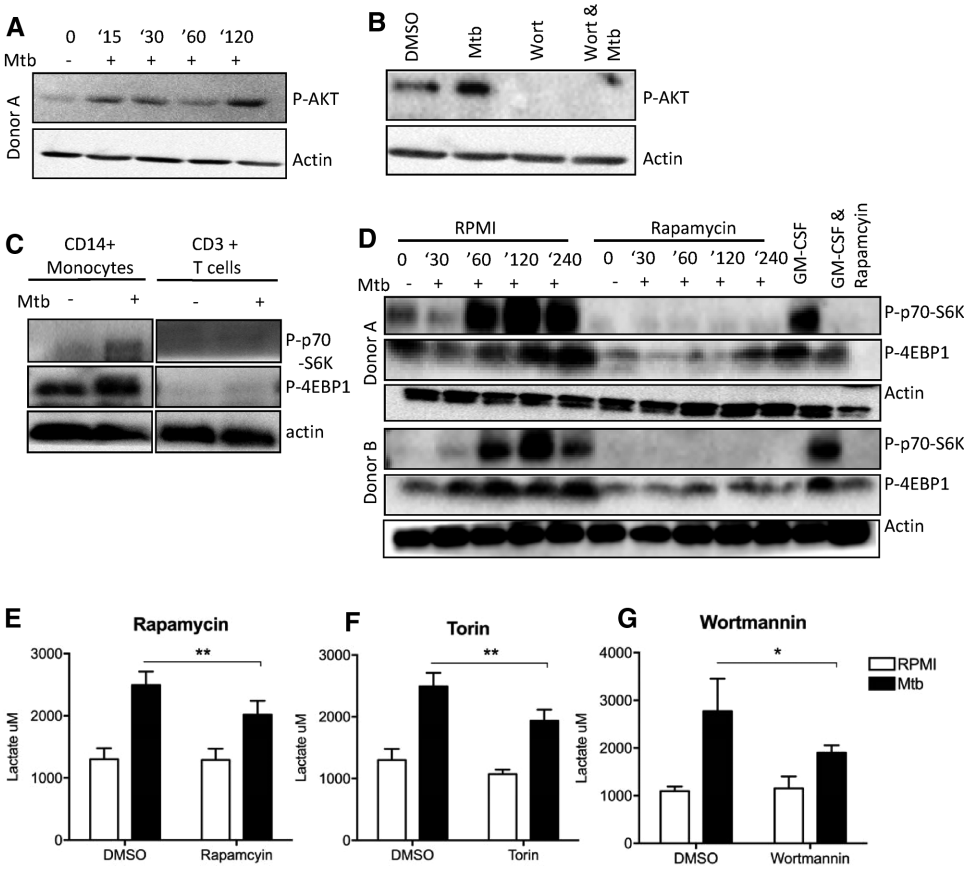

Figure 3. Induction of glycolysis in human PBMCs is mediated by the AKT-mTOR pathway. (A–D) PBMCs were stimulated with RPMI or Mtb in a time-dependent manner in the presence or absence of DMSO (vehicle control), wortmannin (PI3K/AKT inhibitor), or rapamycin (mTOR inhibitor). (C) $CD14^+$ and $CD3^+$ T cells were separated from PBMCs stimulated for 2 h with Mtb. Where indicated, GM-CSF stimulation was included as a positive control. (A, B) AKT, (C, D) p70-S6K and 4E-BP1 phosphorylation and actin levels were determined by Western blot using specific antibodies. (A, B) Cell lysates were harvested at 15, 30, 60, and 120 min poststimulation. (C, D) Cell lysates were harvested at 30, 60, 120, and 240 min poststimulation. Representative blots from two of four donors are shown. (E–G) PBMCs were preincubated with 10 nM rapamycin, 100 nM torin, or 100 nM wortmannin for 1 h prior to stimulation with Mtb lysate. Data are shown as means ± SEM of $n = 9$, pooled from three independent experiments. Means were compared using the Wilcoxon signed-rank test ($^*p < 0.05$, $^{**}p < 0.01$).

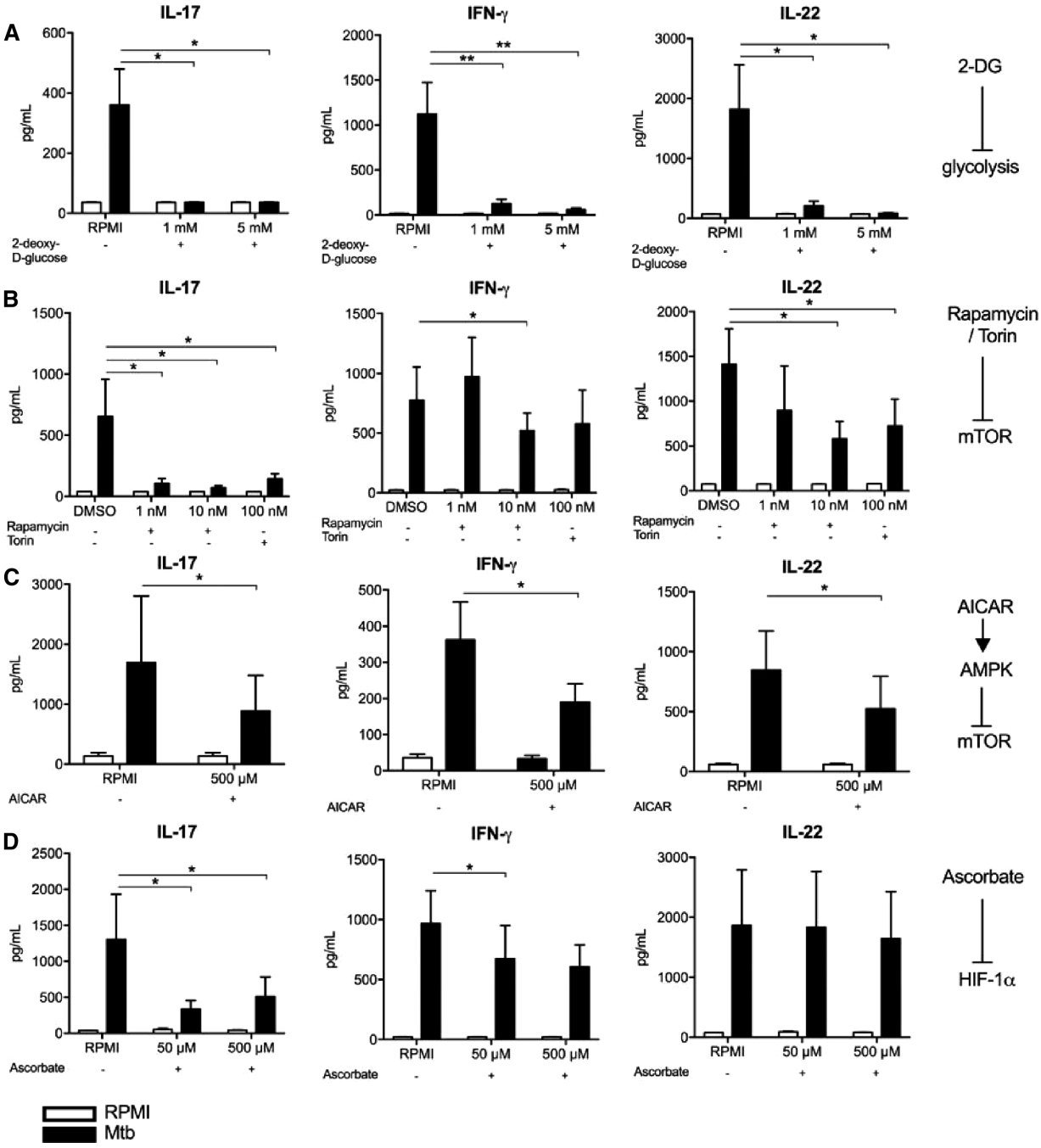

Figure 4. mTOR regulation of Mtb-induced T-cell cytokine responses. (A–D) PBMCs were preincubated with DMSO (vehicle control) or (A) 1 mM or 5 mM 2-deoxy-glucose, (B) 1 nM or 10 nM rapamycin, 100 nM torin, (C) 500 μM AICAR, or (D) 50 μM or 500 μM ascorbate or for 1 h prior to stimulation with Mtb lysate. IL-17, IFN-γ, and IL-22 levels were measured from culture supernatants by ELISA. Data are shown as means ± SEM of $n = 6–9$ pooled from three independent experiments. Means were compared using the Wilcoxon signed-rank test ($^*p < 0.05$, $^{**}p < 0.01$).

with rapamycin or control vehicle 1 day before aerosol infection with Mtb and thereafter daily for 28 days (Fig. 7A). At 28 day postinfection, ex vivo stimulations of splenocytes with Mtb lysate, PPD, PHA, and LPS revealed a potent reduction in the capacity of the rapamycin-treated mice to respond to both Mtb lysate (Fig. 7B) and nonspecific stimuli such as PPD, PHA, and LPS (Supporting Information Fig. 6A–V). Notably, the production of the T_H-derived cytokines IFN-γ and IL-17 was inhibited by rapamycin (Fig. 7B), as previously observed in vitro. Systemic inhibition of mTOR also led to the inhibition of proinflammatory cytokines IL-12 p70 and TNF-α (Fig. 7B). It is highly likely that due to the antimycobacterial effects of rapamycin [17], rapamycin injections did not affect Mtb outgrowth (Supporting Information Fig. 6W).

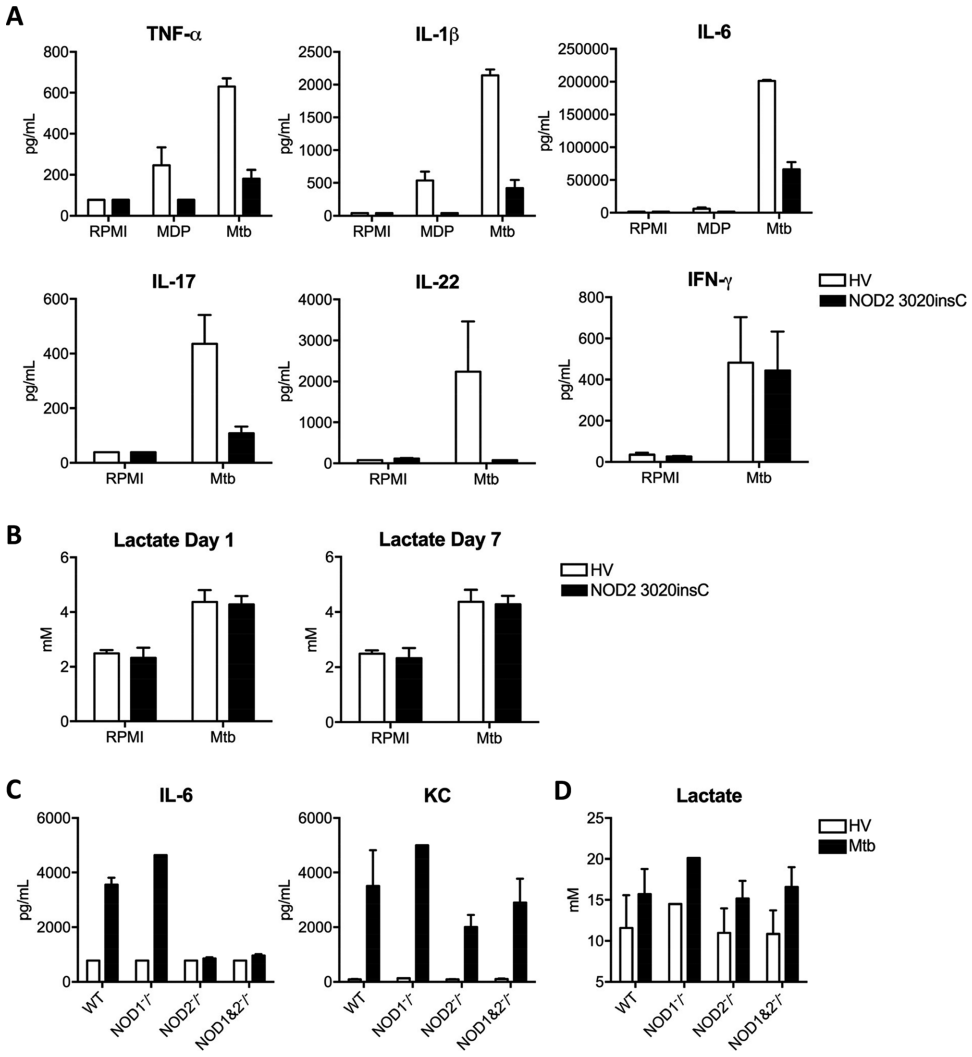

Figure 5. Role of NOD2 in the induction of glycolysis. (A, B) PBMCs from NOD2-deficient patients ($n = 2$) and healthy volunteers ($n = 4$) were stimulated with RPMI, MDP, and Mtb for 24 h and 7 days. The levels of (A) indicated cytokines or (B) lactate production were measured from culture supernatants by ELISA and an enzymatic couple assay, respectively. Data are shown as means ± SEM of the indicated number of donor samples and are from a single experiment. (C, D) BMDMs from WT, NOD1 knockout ($^{-/-}$), NOD2 knockout ($^{-/-}$), and NOD 1/2 double knockout ($^{-/-}$) mice were stimulated with RPMI or 1 μg/mL Mtb lysate for 24 h ($n = 2$). The levels of (C) IL-6 and KC and (D) lactate production were measured as described above. Data are shown as means ± SEM of $n = 2$ from a single experiment.

Discussion

A metabolic switch to aerobic glycolysis, also known as the Warburg effect, was first described by Otto Warburg in cancer cells [18]. In recent years an increasing body of literature has shown that a similar pattern of metabolic rewiring is important for differentiation of effector T_H lymphocytes [5], activation of macrophages and DCs [1] and more recently for Mtb infection [7, 8]. Expanding on this, we used transcriptome data to demonstrate that this switch takes place in patients with active TB disease and we thereafter performed functional experiments to identify the molecular mechanisms governing this switch to glycolysis. Specifically, we show that the switch to glycolysis in cells that encounter Mtb relies on TLR2 recognition and is in part dependent on the intracellular AKT-mTOR axis.

Aerobic glycolysis is an ancient process for generating ATP seen even in early single-cell eukaryotes such as yeast. Although primitive in comparison to the TCA cycle and oxidative phosphorylation, aerobic glycolysis rapidly facilitates the high bioenergetic needs of cells responding to intruding pathogens. We show that this metabolic switch is also necessary for cells to mount an efficient response to Mtb.

The mTOR regulatory complex has been highly conserved throughout evolution. It integrates extracellular and intracellular signals to regulate cell growth, metabolism, proliferation, and survival. The mTOR protein can form two distinct multiprotein complexes: mTOR complex 1 (mTORC1) and mTOR complex 2 (mTORC2). Mtb stimulation increased mTORC1 activity as measured by an increase in phosphorylation of its targets 4E-BP1 and p70-S6K1. Additionally, rapamycin inhibits mTORC1 but cannot

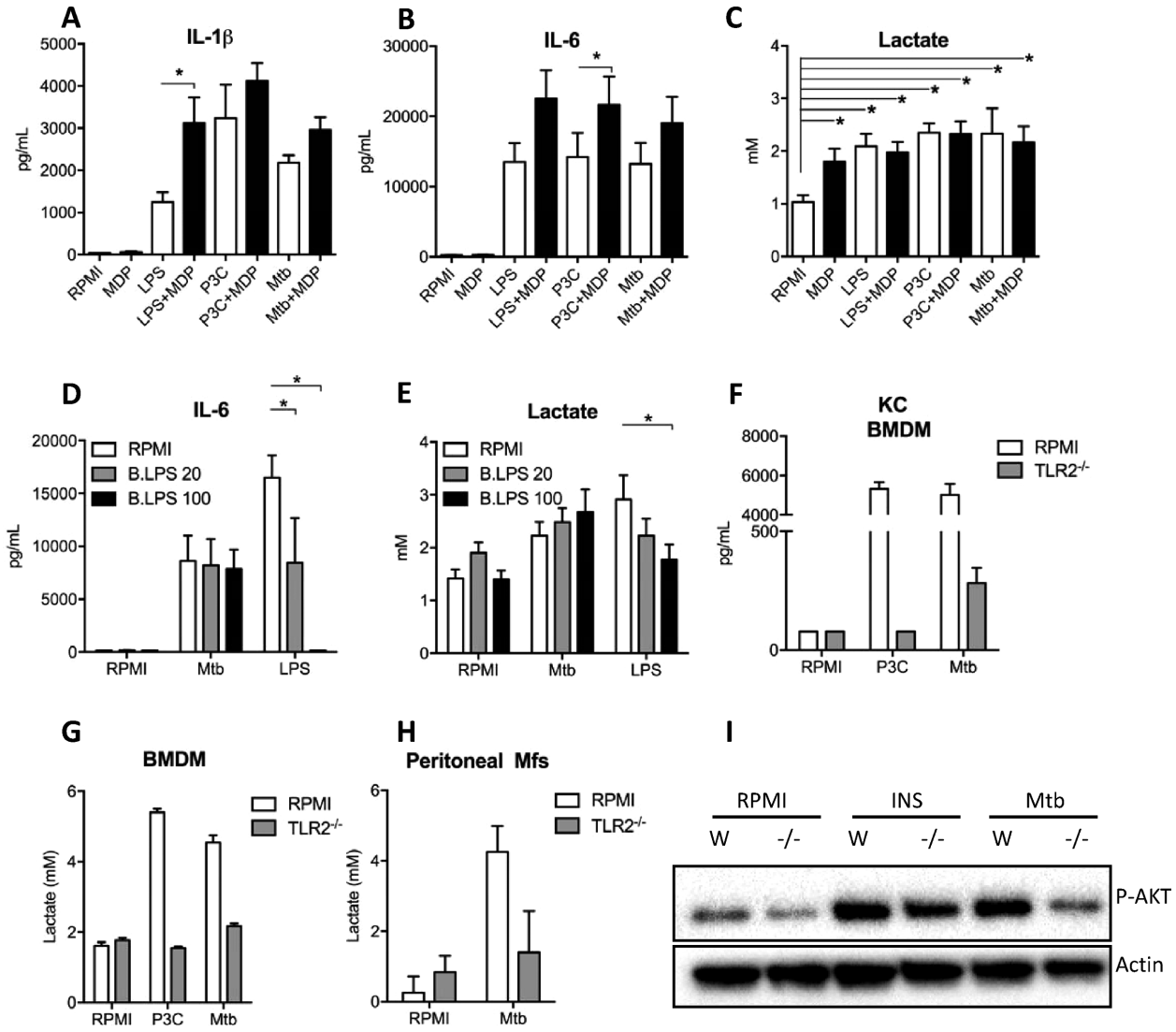

Figure 6. Stimulation via TLR2 initiates rewiring of cellular metabolism in mouse macrophages. (A–C) PBMCs from healthy volunteers ($n = 6$) were stimulated with RPMI, MDP ± LPS, Pam3Cys (P3C) or Mtb lysate for 24 h. The levels of (A) IL-1β, (B) IL-6, and (C) lactate in cell culture supernatants were measured as described above. Data are shown as means ± SEM of $n = 6$ pooled from two experiments. Means were compared using the Wilcoxon signed-rank test (*$p < 0.05$). (D, E) PBMCs were preincubated with TLR4 antagonist *B. quintana* LPS (20 and 100 ng/mL) prior to stimulation with RPMI, Mtb lysate, or LPS. The levels of (D) IL-6 production and (E) lactate in culture supernatants were determined by ELISA and a coupled enzymatic assay, respectively. Data are shown as means ± SEM of $n = 6$–8 pooled from three experiments. Means were compared using the Wilcoxon signed-rank test (*$p < 0.05$). (F–H) BMDMs and peritoneal macrophages (Mfs) from TLR2 knockout ($TLR2^{-/-}$) mice were stimulated with RPMI, P3C (positive control) and Mtb lysate. The levels of (F) KC (IL-8) and (G, H) lactate in culture supernatants were measured by ELISA and a coupled enzymatic assay. Data are shown as means ± SEM of $n = 3$–6 pooled from two experiments. Means were compared using the Wilcoxon signed-rank test. (I) Levels of AKT activation from $TLR2^{-/-}$ BMDMs stimulated with RPMI, insulin (control; INS) and Mtb lysate (Mtb) was determined by western blot. Actin was used as loading control. One of two representative blots is shown.

physically interact or acutely inhibit mTORC2. This suggests that the Mtb-induced switch to aerobic glycolysis is in part due to mTORC1 activation. The involvement of mTORC1 is further supported by studies showing that naive T-helper cells preserve their ability to differentiate into T_H1 and T_H17 cells in the absence of mTORC2 signaling, but not in the absence of mTORC1 signaling [19]. Mechanistically, it would be highly interesting to determine whether mTORC2-deficient cells could commit to glycolysis. Of note, blockade by rapamycin, torin, and wortmannin individually does not completely ablate lactate production suggesting redundancy of these regulators, regulation by other pathways, or incomplete pharmacological inhibition. Dissecting whether the mTOR/AKT pathway is the sole regulator of glycolysis would therefore be of future interest.

NOD2 and TLR receptors are major PRRs for Mtb, with synergistic effects on Mtb-medicated cytokine production [20, 21]. It is thus interesting that rewiring of cellular glucose metabolism is strictly TLR2 dependent (but NOD2 independent), and that the NOD2 agonist MDP does not potentiate TLR2-induced lactate production. The discrepancy between the effects of NOD2 on cytokine

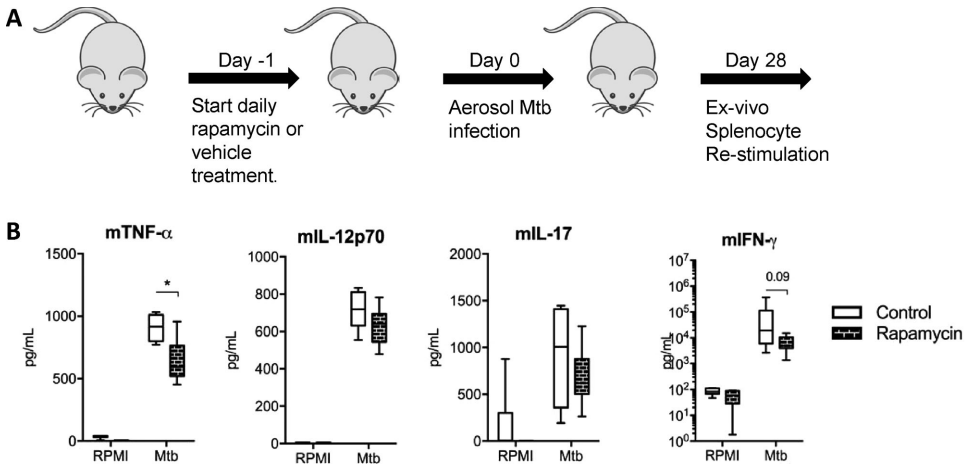

Figure 7. In vivo effects of mTOR inhibition. (A, B) C57/BL6 mice were treated with rapamycin or vehicle (mixed PBS/100% EtOH) from 1 day prior to aerosol infection with Mtb until 28 days postinfection. Mice were euthanized and splenocytes were harvested and restimulated with Mtb lysate (1 μg/mL) for 6 days, after which (B) a bead-based immunoassay for mTNF-α, mIL-12p70, mIIL-17, and mIFN-γ was performed. Data are shown as means ± SEM of $n = 6$ samples from a single experiment. Means were compared using the Mann–Whitney U test ($^*p < 0.05$).

responses and induction of glycolysis suggests the presence of distinct intracellular pathways responsible for these two processes. While NOD2 stimulation is known to induce MAPK activation and NF-kB translocation leading to cytokine induction [22], activation of the AKT/mTOR pathway is not demonstrated. In contrast, TLRs induce both MAPK, NF-κB, and the AKT/mTOR pathway [23, 24]. Moreover, activation of AKT inhibits the NOD2-mediated NF-κB pathway [25], while NOD1 stimulation (that activates similar intracellular pathways) inhibits AKT phosphorylation induced by insulin [26]. These data strongly suggest a fundamental difference between TLRs and NOD2 for activation of AKT/mTOR pathway, with NOD2 unable to induce AKT activation and thus metabolic reprogramming. Future studies that compare this requirement for TLR2 in other infectious stimuli, such as Gram positive or negative bacteria, would be of interest.

T_H cells exert different effector functions and thus it is not surprising that they exhibit distinct metabolic programs. T-effector cells primarily rely on mTOR-driven aerobic glycolysis for energy, while regulatory T cells rely on lipid oxidation and mitochondrial respiration mediated by AMPK [1]. Mtb-induced T_H17 cells appear to be more dependent on aerobic glycolysis than T_H1 cells, possibly due to the upregulation of HIF-1α [27]. HIF-1α is a hypoxia-induced transcription factor that directly controls gene expression of enzymes in the glycolysis pathway [28]. The role of HIF-1α in the generation of IFN-γ-producing T_H1 cells is unclear, as either enhanced or no differences in IFN-γ production have been observed in experimental models lacking HIF-1α [29, 30]. The use of ascorbate, an HIF-1α inhibitor, emulates these observations, as a significant decrease in IL-17 but not IFN-γ production was found in PMBCs.

In vitro inhibition of mTOR with rapamycin or torin led to either no differences or an increase in TNF-α, IL-6, and IL-1β production, in line with literature showing that mTOR inhibits proinflammatory cytokine production via negative regulation of NF-κB, while inhibiting T-cell proliferation [31]. Nonetheless, in our in vivo Mtb infection model, prolonged exposure to rapamycin inhibited overall cytokine responses to Mtb including proinflammatory cytokines such as IL-12 and TNF-α. Likewise, 2-DG, a direct competitive inhibitor of glycolysis, inhibited both monocyte and T-cell-derived cytokines. As mentioned above, the HIF-1α inhibitor ascorbate did not influence monocyte-derived cytokines, in contrast to a previous study showing HIF-1α-dependent LPS-mediated IL-1β production in murine macrophages [32]. This may be explained by the differences in required doses of ascorbate, or discrepancies between human and mouse glucose metabolic processes.

In this study, we take a step further in dissecting the role of leukocyte energy metabolism in the immune responses to Mtb in vitro and in vivo. Recognition of the fact that metabolic rewiring toward glycolysis is crucial for host immunity leads to the hypothesis that perturbations in leukocyte metabolism could be detrimental for the host. For instance, impaired glucose metabolism in patients with diabetes leading to reduced capacity to mount the necessary metabolic changes to respond to Mtb may contribute significantly to their increase in TB susceptibility.

In conclusion, our study has cemented glycolysis as a fundamental process that underpins the cellular circuitry needed to mount effective host responses to Mtb and promotes it as a therapeutic target in TB. In particular, pharmacologic manipulation of enzymes in these pathways may generate more robust and effective immune responses and thus open up new avenues for host-directed therapies for tuberculosis.

Materials and methods

Healthy volunteers

PBMCs were isolated from EDTA tubes or buffy coats obtained after informed consent of healthy volunteers (Sanquin Bloodbank, Nijmegen, Netherlands). As donations were anonymous, no

tuberculosis skin tests or IFN-γ release assay was performed. The incidence of tuberculosis in the Dutch population is extremely low (1.5/100 000), and Bacillus Calmette-Guérin (BCG) vaccination is not part of the routine vaccination program. Experiments were conducted according to the principles expressed in the Declaration of Helsinki.

Isolation of PBMCs, CD14$^+$ Monocytes and CD3$^+$ T cells

Isolation of PBMCs was performed as described previously [33]. CD14$^+$ monocytes or CD3$^+$ T cells were purified from freshly isolated PBMCs using MACS microbeads by positive selection according to the manufacturer's instructions (Miltenyi Biotec, Germany).

Stimulation experiments

For stimulation experiments, 5×10^6 PBMCs/mL or 1×10^6 monocytes/mL were stimulated with RPMI, 1 μg/mL Mtb strain H37Rv (Mtb) lysate, 10 μg/mL Pam3Cys (EMC Microcollections, Germany) and/or 10 μg/mL MDP (Sigma) in the presence or absence of 1 or 10 nM rapamycin (LC-laboratories), 100 nM Torin (Tocris), 50 or 500 μM sodium L-ascorbate (Sigma), 50 or 500 μM AICAR (Brunschwig chemie), 100 nM wortmannin (Cayla Invivogen), or 20 or 100 ng/mL of TLR4 inhibitory ligand double-extracted *B. quintana* LPS for 24 h or with 10% pooled human serum for 7 days. PBMCs from patients with the homozygous carriage of a frameshift in *Nod2* due to an insertion of cysteine at position 1007 (1007finsC) (rs2066847) were stimulated with RPMI, MDP, or Mtb for 1 or 7 days. Culture supernatants were collected and stored at −20°C. For Western blots, 5×10^6 PBMCs were stimulated with RPMI, 1 μg/mL Mtb lysate or 50 ng/mL GM-CSF in the presence or absence of the aforementioned inhibitors. Cytokine measurements from cell culture supernatants were performed by ELISA namely IL-1β, TNF-α, IL-17A, IL-22 (R&D Systems, Minneapolis, MN); and IL-6, IFN-γ, and IL-10 (Sanquin, Amsterdam) were measured.

Animal experiments

TLR2 knockout mice were kindly provided by Prof S. Akira (Department of Host Defense, Research Institute for Microbial Diseases, Osaka University, Osaka, Japan) and were fully backcrossed to the C57BL/6 background. Age- and sex-matched control C57BL/6 mice were obtained from Charles River Wiga (Sulzfeld, Germany).

Wild-type, NOD1, NOD2, and NOD1/NOD2 double knockout mice were bred and maintained in the St. Jude Children's Research Hospital (Memphis, TN). After dissection of mouse legs, the BM was flushed out using sterile PBS and cells obtained were differentiated over a period of 7 days0 at 37°C, 5% CO_2 in Dulbecco's modified Eagle's medium (DMEM; Gibco, Invitrogen, Carlsbad, CA, USA) supplemented with 30% L929 medium, 10% heat-inactivated filtered foetal bovine serum (Invitrogen), 1% nonessential amino acids (Life Technologies), 100 U/mL penicillin and 100 mg/mL streptomycin. On day 6 BMDMs were washed, counted, and seeded in 96-well plates at a concentration of 1×10^5 cells/well or in 6-well plates at 1×10^6 cells/well for Western blotting. Cells were left to rest overnight at 37°C, after which they were stimulated with medium, namely 10 μg/mL Pam3Cys, 1 μg/mL Mtb or 100 nM insulin. Experiments were approved by the Ethics Committee on Animal Experimentation of the Radboud University Medical Center and protocols were approved by the St. Jude Children's Research Hospital Committee on the Use and Care of Animals.

Female 8- to 10-week-old C57BL/6 mice were kept under pathogen-free conditions at the Max Planck Institute for Infection Biology in Berlin, Germany (ethical approval of the Berlin Office for Health and Social Affairs reference number G 0179/12). Mtb strain H37Rv was grown in Middlebrook 7H9 broth (BD Biosciences) supplemented with 0.2% glycerol, 0.05% Tween 80, and 10% ADC enrichment (BD Biosciences) until it reached a mid-logarithmic growth phase and then stored at –80°C. Animals were aerosol infected with 200 CFUs using a Glas-Col inhalation exposure system. Rapamycin (Sigma) or vehicle (PBS/100% EtOH) was injected the day before aerosol infection and thereafter daily for 28 days. Splenocytes were isolated from single-cell suspensions prepared by mechanical dissociation through a 70 μm nylon mesh in RPMI 1640 medium with 10% foetal calf serum (Gibco). Splenocytes were seeded in a 24-well-plate at a concentration of 2.5×10^6 cells /mL and stimulated with 1 μg/mL of Mtb lysate, 1 μg/mL of PPD (Staten Serum Institut, Copenhagen), 10 μg/mL PHA (Sigma) or 10 ng/mL of LPS (from *E. coli* 055:B5, Sigma). After 6 days supernatants were collected and stored at –20°C. Cytokines were analyzed using a bead-based assay (Bio-Rad).

Metabolite measurements

Lactate was measured from cell culture supernatants using a coupled enzymatic assay in which lactate was oxidized and the resulting H_2O_2 was coupled to the conversion of Amplex Red reagent to fluorescent resorufin by HRP (horseradish peroxidase) [34]. Measurement of the NAD$^+$/NADH redox ratio was adapted from Zhu et al. [35]. Glucose consumption was measured according to the manufacturer's instructions using the Amplex Red Glucose/Glucose Oxidase Assay Kit (Life Technologies).

Real-time analysis of the ECAR and the OCR on CD14+ monocytes was performed using an XF-96 Extracellular Flux Analyzer (Seahorse Bioscience). Briefly, monocytes were plated in XF-96 cell culture plates (2×10^5 monocytes/well) in the presence of RPMI or Mtb lysate for 24 h in 10% human pooled serum. The monocytes were washed and analyzed in XF Base Medium (unbuffered DMEM with 25 mM glucose and 2 mM L-glutamine, pH was adjusted to 7.4). Basal OCR and ECAR of the monocytes was measured every 5 min for 20 min in total.

Cell viability assessment

The percentage of cells that underwent early or late apoptosis was determined by labeling with annexin V–fluorescein isothiocyanate (FITC, Biovision) and staining with propidium iodide (PI, Sigma Aldrich), according to the manufacturer's instructions. Briefly, stimulated PBMCs were resuspended in 200 μL of RPMI and incubated on ice in the dark with 1 μL of Annexin V-FITC for 15 min followed by a 5 min incubation with 1.5 μL of PI. The relative level of apoptotic cells was detected by flow cytometry within 1 h, using a FC500 flow cytometer (Beckman Coulter) and data were analyzed using Kaluza 1.3 software (Beckman Coulter).

Western blotting

Western blotting was carried out using a Trans Turbo Blot system (Bio-Rad) according to the manufacturer's instructions. A total of 5×10^6 PBMCs or 1×10^6 $CD14^+$ monocytes or 1×10^6 $CD3^+$ T cells were lysed in 100 μL lysis buffer. The cell homogenate was frozen, thawed, and processed for Western blot analysis. Equal amounts of protein were resolved by SDS-PAGE on 4–15% polyacrylamide gels (Bio-Rad). Separated proteins were transferred to PVDF (Bio-Rad) membranes. According to the manufacturer's instructions, the membrane was blocked for 1 h and then incubated overnight with a primary antibody at a dilution of 1:1000 in 5% w/v bovine serum albumin (BSA, Sigma) or milk in TBS-Tween buffer (TBS-T). After overnight incubation, blots were washed in TBS-T three times and incubated with HRP-conjugated anti-rabbit antibody (1:5000; Sigma) in 5% w/v milk in TBS-T for 1 h at RT. After washing the blots were developed with ECL (Bio-Rad) according to the manufacturer's instructions. The primary antibodies used were rabbit anti-actin (Sigma), mAB phospho-p70 S6 Kinase (Thr389) (Cell Signalling), phospho-AKT (Cell Signalling), and phospho-4EBP1 (Cell Signalling).

Transcriptome analyses

We obtained previously published transcriptome data for our analysis (GSE42606) [36] Briefly, PBMCs were stimulated with RPMI or Mtb (1 μg/mL) for 24 h at 37°C and 5% CO_2. Total RNA was extracted in 800 μL of TRIzol reagent (Invitrogen). Global gene expression was profiled using an Illumina Human HT-12 Expression BeadChip according to the manufacturer's instructions. Image analysis, bead-level processing, and quantile normalisation of array data were performed using the Illumina LIMS platform, BeadStudio. The quantile normalized expression data for glycolysis and TCA cycle genes (derived from KEGG pathway) were extracted to perform differential expression analysis between RPMI and Mtb stimulations.

Human gene expression analysis

Publicly available microarray data (Illumina Human HT-12 V3 BeadChip) from cohorts of patients with active and latent tuberculosis and uninfected controls in the UK and South Africa [9]) were obtained from the Gene Expression Omnibus (GEO) under accession number GSE19491. We restricted our analysis to the expression data from whole blood (collected in Tempus tubes, Applied Biosystems) from the UK test cohort and the South-African validation cohort. Genes implicated in glycolysis (path:hsa00010) and TCA cycle (path:hsa00020) pathways were extracted from KEGG, putative genes were removed and the remaining genes were converted into Illumina probe numbers using DAVID [37, 38]. Probes that had a negative expression for one of the samples were excluded.

Statistical Analysis

Principal component analysis was performed on log-transformed data using singular value decomposition separately for the glycolysis and TCA cycle pathways in Python. Scores of the samples projected on principal component (PC) 1 for glycolysis were plotted against the scores on PC1 for the TCA cycle, to show the maximum combined variance of both pathways in one graph. Additionally, binary regression analysis was performed on the scores projected on PC1 for both pathways with LTBI (0) versus PTB (1) for the South-African cohort in SPSS 21.

The heat maps show differences in expression based on $\log_2$ transformed data from the different groups. Statistical testing of the in vitro data set was performed on the mean expression between the unstimulated (RPMI) and stimulated (Mtb) samples using a Wilcoxon signed-rank test for parametric data; adjusted p-values less than 0.05 were considered significant. LTBI versus PTB patients were compared using Mann–Whitney U tests. Color coding was based on the minimum and maximum for each of the comparisons. In the legend, changes were transformed back for interpretability. Genes that showed a differential expression in any of the datasets are presented in the figure.

Differences in cytokine production were analyzed using the Wilcoxon signed-rank test for nonparametric distributions. Data were considered statistically significant at a p-value < 0.05. Data are shown as cumulative results of levels obtained in all volunteers (means ± SEM).

Acknowledgements: This study was supported by The European Union's Seventh Framework Programme (EU FP7) project TANDEM (HEALTH-F3-2012-305279). M.G.N. was supported by a Vici Grant of the Netherlands Organization for Scientific Research and by an ERC Starting Grant (ERC No. 310372). R.v.C. was supported by a Vidi grant from the Netherlands Organization for

Scientific Research (No. 91710310). T.H.M.O. was supported by The Netherlands Organization for Scientific Research (NWO-TOP grant), EC HORIZON2020 TBVAC2020 (contract no. 643381). X.W. was supported by NSFC 11101321 and NSFC 61263039.

Conflict of interest: The authors declare no financial or commercial conflict of interest.

References

1 **Michalek, R. D., Gerriets, V. A., Jacobs, S. R., Macintyre, A. N., MacIver, N. J., Mason, E. F., Sullivan, S. A. et al.**, Cutting edge: distinct glycolytic and lipid oxidative metabolic programs are essential for effector and regulatory CD4(+) T-cell subsets. *J. Immunol.* 2011. **186**: 3299–3303.

2 **Cheng, S. C.**, mTOR- and HIF-1 alpha-mediated aerobic glycolysis as metabolic basis for trained immunity. *Science* 2014. **346**: 1579–1589.

3 **Pearce, E. L., Walsh, M. C., Cejas, P. J., Harms, G. M., Shen, H., Wang, L. S., Jones, R. G. et al.**, Enhancing CD8 T-cell memory by modulating fatty acid metabolism. *Nature* 2009. **460**: U103–U118.

4 **Everts, B., Amiel, E., Huang, S. C. C., Smith, A. M., Chang, C. H., Lam, W. Y., Redmann, V. et al.**, TLR-driven early glycolytic reprogramming via the kinases TBK1-IKK epsilon supports the anabolic demands of dendritic cell activation. *Nat. Immunol.* 2014. **15**: 323–332.

5 **Krawczyk, C. M., Holowka, T., Sun, J., Blagih, J., Amiel, E., DeBerardinis, R. J., Cross, J. R. et al.**, Toll-like receptor-induced changes in glycolytic metabolism regulate dendritic cell activation. *Blood* 2010. **115**: 4742–4749.

6 **Waickman, A. T. and Powell, J. D.**, mTOR, metabolism, and the regulation of T-cell differentiation and function. *Immunol. Rev.* 2012. **249**: 43–58.

7 **Gleeson, L. E., Sheedy, F. J., Palsson-McDermott, E. M., Triglia, D., O'Leary, S. M., O'Sullivan, M. P., O'Neill, L. A. et al.**, Cutting edge: mycobacterium tuberculosis induces aerobic glycolysis in human alveolar macrophages that is required for control of intracellular bacillary replication. *J. Immunol.* 2016. **196**: 2444–2449.

8 **Shi, L., Salamon, H., Eugenin, E. A., Pine, R., Cooper, A. and Gennaro, M. L.**, Infection with Mycobacterium tuberculosis induces the Warburg effect in mouse lungs. *Sci. Rep.* 2015. **5**: 18176.

9 **Berry, M. P., Graham, C. M., McNab, F. W., Xu, Z., Bloch, S. A., Oni, T., Wilkinson, K. A. et al.**, An interferon-inducible neutrophil-driven blood transcriptional signature in human tuberculosis. *Nature* 2010. **466**: 973–977.

10 **Ganeshan, K. and Chawla, A.**, Metabolic regulation of immune responses. *Annu. Rev. Immunol.* 2014. **32**: 609–634.

11 **Everts, B., Amiel, E., van der Windt, G. J. W., Freitas, T. C., Chott, R., Yarasheski, K. E., Pearce, E. L. et al.**, Commitment to glycolysis sustains survival of NO-producing inflammatory dendritic cells. *Blood* 2012. **120**: 1422–1431.

12 **Laplante, M. and Sabatini, D. M.**, mTOR signaling at a glance. *J. Cell Sci.* 2009. **122**: 3589–3594.

13 **Reif, K., Burgering, B. M. and Cantrell, D. A.**, Phosphatidylinositol 3-kinase links the interleukin-2 receptor to protein kinase B and p70 S6 kinase. *J. Biol. Chem.* 1997. **272**: 14426–14433.

14 **Burgering, B. M. and Coffer, P. J.**, Protein kinase B (c-Akt) in phosphatidylinositol-3-OH kinase signal transduction. *Nature* 1995. **376**: 599–602.

15 **Kleinnijenhuis, J., Oosting, M., Joosten, L. A., Netea, M. G. and Van Crevel, R.**, Innate immune recognition of Mycobacterium tuberculosis. *Clin. Dev. Immunol.* 2011. **2011**: 405310.

16 **Popa, C., Abdollahi-Roodsaz, S., Joosten, L. A., Takashi, N., Sprong, T., Matera, G., Liberto, M. C. and Foca, Alfredo**, Bartonella quintana Lipopolysaccharide Is a Natural Antagonist of Toll-Like Receptor. *Infect Immun.* 2007. **75**: 4831–4837.

17 **Zullo, A. J., Smith, K. L. J. and Lee, S.**, Mammalian target of rapamycin inhibition and mycobacterial survival are uncoupled in murine macrophages. *BMC Biochem.* 2014. **4**: 15.

18 **Warburg, O., Wind, F. and Negelein, E.**, The metabolism of tumors in the body. *J. Gen. Physiol.* 1927. **8**: 519–530.

19 **Delgoffe, G. M., Pollizzi, K. N., Waickman, A. T., Heikamp, E., Meyers, D. J., Horton, M. R., Xiao, B. et al.**, The kinase mTOR regulates the differentiation of helper T cells through the selective activation of signaling by mTORC1 and mTORC2. *Nat. Immunol.* 2011. **12**: 295–303.

20 **Reiling, N., Holscher, C., Fehrenbach, A., Kroger, S., Kirschning, C. J., Goyert, S. and Ehlers, S.**, Cutting edge: Toll-like receptor (TLR)2- and TLR4-mediated pathogen recognition in resistance to airborne infection with Mycobacterium tuberculosis. *J. Immunol.* 2002. **169**: 3480–3484.

21 **Drennan, M. B., Nicolle, D., Quesniaux, V. J., Jacobs, M., Allie, N., Mpagi, J., Fremond, C. et al.**, Toll-like receptor 2-deficient mice succumb to Mycobacterium tuberculosis infection. *Am. J. Pathol.* 2004. **164**: 49–57.

22 **Caruso, R., Warner, N., Inohara, N. and Nunez, G.**, NOD1 and NOD2: signaling, host defense, and inflammatory disease. *Immunity* 2014. **41**: 898–908.

23 **O'Neill, L. A., Golenbock, D. and Bowie, A. G.**, The history of Toll-like receptors - redefining innate immunity. *Nat. Rev. Immunol.* 2013. **13**: 453–460.

24 **Kawai, T. and Akira, S.**, The role of pattern-recognition receptors in innate immunity: update on Toll-like receptors. *Nat. Immunol.* 2010. **11**: 373–384.

25 **Zhao, L., Lee, J. Y. and Hwang, D. H.**, The phosphatidylinositol 3-kinase/Akt pathway negatively regulates Nod2-mediated NF-kappa B pathway. *Biochem. Pharmacol.* 2008. **75**: 1515–1525.

26 **Zhou, Y. J., Zhou, H., Li, Y. and Song, Y. L.**, NOD1 activation induces innate immune responses and insulin resistance in human adipocytes. *Diabetes Metab.* 2012. **38**: 538–543.

27 **Shi, L. Z., Wang, R. N., Huang, G. H., Vogel, P., Neale, G., Green, D. R. and Chi, H. B.**, HIF1 alpha-dependent glycolytic pathway orchestrates a metabolic checkpoint for the differentiation of T(H)17 and T-reg cells. *J. Exp. Med.* 2011. **208**: 1367–1376.

28 **Iyer, N. V., Kotch, L. E., Agani, F., Leung, S. W., Laughner, E., Wenger, R. H., Gassmann, M. et al.**, Cellular and developmental control of O_2 homeostasis by hypoxia-inducible factor 1 alpha. *Genes Dev.* 1998. **12**: 149–162.

29 **Guo, J., Lu, W., Shimoda, L. A., Semenza, G. L. and Georas, S. N.**, Enhanced interferon-gamma gene expression in T cells and reduced ovalbumin-dependent lung eosinophilia in hypoxia-inducible factor-1-alpha-deficient mice. *Int. Arch. Allergy Immunol.* 2009. **149**: 98–102.

30 **Dang, E. V., Barbi, J., Yang, H. Y., Jinasena, D., Yu, H., Zheng, Y., Bordman, Z. et al.**, Control of T(H)17/T(reg) balance by hypoxia-inducible factor 1. *Cell* 2011. **146**: 772–784.

31 **Weichhart, T., Costantino, G., Poglitsch, M., Rosner, M., Zeyda, M., Stuhlmeier, K. M., Kolbe, T. et al.**, The TSC-mTOR signaling pathway regulates the innate inflammatory response. *Immunity* 2008. **29**: 565–577.

32 **Tannahill, G. M.**, **Curtis, A. M.**, **Adamik, J.**, **Palsson-McDermott, E. M.**, **McGettrick, A. F.**, **Goel, G.**, **Frezza, C. et al.**, Succinate is an inflammatory signal that induces IL-1 beta through HIF-1 alpha. *Nature* 2013. **496**: 238.

33 **Netea, M. G.**, **Gow, N. A.**, **Munro, C. A.**, **Bates, S.**, **Collins, C.**, **Ferwerda, G.**, **Hobson, R. P. et al.**, Immune sensing of Candida albicans requires cooperative recognition of mannans and glucans by lectin and Toll-like receptors. *J. Clin. Invest.* 2006. **116**: 1642–1650.

34 **Lachmandas, E.**, **van den Heuvel, C. N.**, **Damen, M. S.**, **Cleophas, M. C.**, **Netea, M. G. and van Crevel, R.**, Diabetes mellitus and increased tuberculosis susceptibility: the role of short-chain fatty acids. *J. Diabetes Res.* 2016. **2016**: 6014631.

35 **Zhu, C. T. and Rand, D. M.**, A hydrazine coupled cycling assay validates the decrease in redox ratio under starvation in Drosophila. *PLoS One* 2012. **7**: e47584.

36 **Smeekens, S. P.**, **Ng, A.**, **Kumar, V.**, **Johnson, M. D.**, **Plantinga, T. S.**, **van Diemen, C.**, **Arts, P. et al.**, Functional genomics identifies type I interferon pathway as central for host defense against *Candida albicans*. *Nat. Commun.* 2013. **4**: 1342.

37 **Huang, D. W.**, **Sherman, B. T. and Lempicki, R. A.**, Systematic and integrative analysis of large gene lists using DAVID bioinformatics resources. *Nat. Protoc.* 2009. **4**: 44–57.

38 **Huang, D. W.**, **Sherman, B. T. and Lempicki, R. A.**, Bioinformatics enrichment tools: paths toward the comprehensive functional analysis of large gene lists. *Nucleic Acid Res.* 2009. **37**: 1–13.

Abbreviations: **CON**: healthy controls · **ECAR**: extracellular acidification rate · **LTBI**: latent tuberculosis infection · **MDP**: muramyl dipeptide · **Mtb**: Mycobacterium tuberculosis · **mTOR**: mammalian target of rapamycin · **OCR**: oxygen consumption rate · **PTB**: pulmonary TB patients · **TCA**: tri-carboxylic acid cycle

Full correspondence: Dr. Mihai G. Netea, Department of Medicine, Radboud University Nijmegen Medical Centre, Geert Grooteplein Zuid 8, 6525 GA Nijmegen, The Netherlands
e-mail: mihai.netea@radboudumc.nl

Received: 18/12/2015
Revised: 12/7/2016
Accepted: 17/8/2016
Accepted article online: 14/9/2016